Reactive & Functional Polymers 69 (2009) 698–704

Contents lists available at ScienceDirect

Reactive & Functional Polymers

journal homepage: www.elsevier.com/locate/react

UV curable sulfonated hybrid materials and their performance as proton exchange membranes

M. Gurtekin [a], N. Kayaman-Apohan [a,*], M.V. Kahraman [a], Y. Menceloglu [b], A. Gungor [a]

[a] Marmara University, Faculty of Art and Science, Department of Chemistry, 34722 Göztepe-İstanbul, Turkey
[b] Sabancı University, Faculty of Engineering and Natural Sciences, 34956 Tuzla-İstanbul, Turkey

ARTICLE INFO

Article history:
Received 23 January 2009
Received in revised form 28 April 2009
Accepted 7 May 2009
Available online 31 May 2009

Keywords:
Sol–gel
2-Acrylamido-2-methylpropane sulfonic acid
UV-curing
Proton conductivity
Fuel cell

ABSTRACT

In this study 2-acrylamido-2-methylpropanesulfonic acid (AMPS) containing UV curable nanocomposite membranes were prepared by using the sol–gel method. Tetraethylorthosilicate (TEOS), and 3-(methacryloyloxy)propyl trimethoxysilane (MAPTMS) were used, respectively as an inorganic precursor and coupling agent. Cross linking agents such as poly(ethylene glycol diacrylate) (PEGMA) and ethylene glycol dimethacrylate (EGDMA) were used to arrange the mechanical and physical properties of the resulting hybrid membrane. The hybrid formulation polymerized under UV irradiation and the gel percentage, water uptake of the membranes were calculated. The polymerization conversion of the organic part was investigated by using photo-differential scanning calorimetry (photo-DSC). The thermal and mechanical properties of the membranes indicated good stability. The morphological structure of membranes was investigated by scanning electron microscopy (SEM). In addition proton conductivity and methanol selectivity measurements were performed. The proton conductivity of the AMPS20–SOLGEL30 nanocomposite membrane is about 0.138 S cm^{-1} at 50 °C. Selectivity toward methanol for the same membrane is very low with a selectivity factor of $\alpha = 0.032$, which satisfies the requirements for DMFC applications.

1. Introduction

Fuel cells have emerged as an alternative power source because of their high-energy conversion efficiency and eco-friendliness [1]. Among the various types of fuel cells, the direct methanol fuel cells (DMFC), where liquid methanol is used directly as the fuel, has the added advantages of safer handling and storage of the fuel, and a simpler overall system design [2]. Nafion® at present is one of the most advanced commercially available membranes for DMFC. Although Nafion® has excellent chemical and mechanical stability and high proton conductivity, it has some disadvantages that restrict its industrial applications such as high cost and high methanol cross-over. Therefore, lower cost membranes with high performance are strongly desired [3].

Many researchers have investigated alternative polymers with hydrocarbon structures including polysulfones [4], poly(ether ether ketone)s, polyimides, and polybenzimidazoles [5–7]. 2-Acrylamido-2-methylpropane sulfonic acid (AMPS) based polyelectrolytes showed good chemical stability, high proton conductivity, and promising application in DMFC. Since AMPS is a water-soluble monomer, it is necessary to copolymerize it with another proper monomer in order to control the swelling. It is known that conductivity increases with water content, but at temperatures exceeding 100 °C it decreases, as water is lost. Walker Jr. et al. reported a cross-linked copolymer of AMPS and 2-hydroxyethyl methacrylate (HEMA) as an alternative membrane material for replacing Nafion® in DMFC [8]. Fumed silicas were also added in an attempt to increase the amount of water adsorbed by the membrane and to enhance water retention. Films composed of 4% AMPS and 96% HEMA had a room temperature proton conductivity of 0.029 S cm^{-1}, which increased to 0.06 S cm^{-1} at 80 °C.

Recently a new methanol-blocking polymer matrix which consists of poly(4-vinylphenol-co-methyl methacrylate), poly(butyl methacrylate), and Paraloid® B-82 acrylic copolymer resins as a methanol barrier phase and AMPS as an embedded proton source has been reported [9]. The choice of AMPS is based on its superior ability to support ion conduction under low water conditions compared with Nafion® [10]. The highest proton conductivity of the AMPS-containing membrane is about 0.030 S cm^{-1} at 70 °C. The low methanol permeability (10^{-8}–10^{-7} cm^2 s^{-1}) of the AMPS-containing membranes is their primary advantage for DMFC applications.

Shen et al. have prepared the copolymers of AMPS and methyl methacrylate by free radical polymerization [11] and these membranes showed higher water uptake, though they had lower ion exchange capacity (IEC) compared with Nafion®-117. The proton conductivity of the membrane with IEC of 0.9 mmol/g was

* Corresponding author. Tel.: +90 216 3479641; fax: +90 216 3478783.
E-mail address: napohan@marmara.edu.tr (N. Kayaman-Apohan).

1381-5148/$ - see front matter © 2009 Elsevier Ltd. All rights reserved.
doi:10.1016/j.reactfunctpolym.2009.05.004

1.14×10^{-2} S cm^{-1} and its methanol permeability coefficient was 5.46×10^{-7} cm^2 s^{-1}, much lower than that of Nafion®-117.

In addition, inorganic–organic composite electrolyte membranes have also been investigated as another approach obtaining low methanol permeability. Kanamura and his coworkers developed a composite electrolyte membrane consisting of a polyelectrolyte gel and an ordered porous silica membrane [12]. It exhibited both high proton conductivity and low methanol crossover due to suppression of polymer expansion by the hard silica matrix. However, the silica matrix has very low proton conductivity, so that only the polyelectrolyte gel electrolyte contributes to the proton conductivity. Recently, they reported a new proton conducting membrane that was prepared by surface sulfonation of three-dimensionally ordered silica [13]. The sulfonic acid groups were introduced by the direct reaction method through a ring-opening reaction of 1,3-propanesulton and the sulfonated silica matrix exhibited high proton conductivity of 6.0×10^{-3} S cm^{-1} at 60 °C under 90% relative humidity. This value was about 400 times higher than that of unmodified silica matrix.

The most widely employed method for preparing hybrid materials is the sol–gel technique, which allows obtaining cross-linked inorganic silica into the polymer network [14]. Hybrid materials can be prepared by a radiation-curing technique such as using a UV curable binder system [15,16]. The UV-curing system is a high-speed process where UV light induces the polymeric film formation leading to a rapid transformation of a wet film into the solid film. It also combines advantages such as low energy consumption and less environmental pollution due to being a solvent free process [17].

The main objective of this work is the development of novel AMPS based UV curable organic/inorganic hybrid membranes to reduce the methanol permeability and obtain high proton conductivity through the membrane. To accomplish this aim, membranes having different compositions of AMPS and AA were prepared, together with sol–gel-derived silica gel. In the hybrid system, AMPS and AA units act as a proton conducting moiety and NVP, PEG dimethacrylate and silica gel matrix provide structural stability and rigidity that should in turn reduce methanol permeability.

2. Experimental

2.1. Materials

The monomers N-vinyl-2-pyrrolidone (NVP, ISP-Turkey), Acrylic acid (AA, Henkel-Turkey), 2-acrylamido-2-methylpropane sulfonic acid (AMPS, Sigma), the crosslinking agents such as poly(ethylene glycol dimethacrylate) (PEGMA, Fluka), ethylene glycol dimethacrylate (EGDMA, Merck), tetraethylorthosilicate (TEOS, Merck), and 3-(methacryloyloxy)propyl trimethoxysilane (MAPTMS, Fluka) and the photoinitiator, 1-hydroxy-cyclohexyl-phenyl-ketone (Irgacure-184, Ciba Specialty Chemicals) were used as received. All the other chemicals were of analytical grade and used without further purification. Deionized water of 18.2 MΩ cm resistivity obtained from a Milli Q-water purification system (Millipore, Anamed-Turkey) was used for the preparation of all solutions.

2.2. Preparation of the sol–gel precursor

The precursor sol was prepared by employing tetraethoxysilane (TEOS) (5.0 g, 0.024 mol) and 3-(methacryloxy)propyl trimethoxysilane (MAPTMS) (6.0 g, 0.024 mol) as the precursor alkoxides, ethanol (EtOH) (2.21 g, 0.048 mol) as solvent, (1.73 g, 0.096 mol) distilled water for hydrolysis and (0.062 g) p-toluene sulfonic acid as a catalyst. All chemicals were of analytical grade and used without further purification. Initially, TEOS, MAPTMS and EtOH were charged into a vessel and then water, which had been acidified by slow addition of p-toluene sulfonic acid into the vessel while stirring continuous at room temperature. The whole mixture was then kept for 12 h under stirring to obtain a silane sol [18].

2.3. Preparation of membranes

The membranes based on N-vinyl-2-pyrrolidone, acrylic acid and 2-acrylamido-2-methylpropane sulfonic acid were synthesized by free radical crosslinking copolymerization with 20 wt% of PEGMA and 3 wt% of EGDMA as crosslinkers. The membranes were prepared by the UV-curing technique and all formulations contained 2 wt% of Irgacure-184 as photoinitiator. Briefly, aqueous NVP, AA and AMPS solutions were prepared in 20 wt% deionized water with various compositions. The required amounts of the sol–gel precursor in the range between 0 and 30 wt% were added into the organic phase. The feed compositions are given in Table 1. The detailed flow chart of the preparation procedure of UV curable organic–inorganic hybrid coating is shown in Scheme 1.

Before the UV-curing process, the solution was purged with nitrogen gas for 15 min to eliminate dissolved oxygen in the system. Then, the total mixture was transferred to Teflon® molds with 50 mm × 10 mm × 1 mm in size. In order to prevent the inhibiting effect of oxygen, the mixture in the mold was covered by transparent 25 μm thick Teflon® film. Finally, the formulations were irradiated for 300 s under high pressure UV lamp (OSRAM 300 W, λ_{max} = 365 nm). The obtained membranes were removed from the mold and cut into pieces that have a 10 mm × 10 mm × 1 mm dimension. The membranes were immersed in a large excess of deionized water for 1 day to wash out any unreacted monomers and initiators and then dried in a vacuum oven at 35 °C for several days until reaching a constant weight [19].

2.4. Characterization

The solid state cross-polarization (CP)/magic-angle spinning (MAS) NMR spectra were recorded using a Bruker Avance Superconducting FT NMR Spectrometer operated at 300 MHz.

Table 1
Composition of the membranes: all formulations contain 20 wt% of PEGMA, 3 wt% of EGDMA as crosslinkers and 2 wt% of photoinitiator.

	AMPS (%)	AA (%)	NVP (%)	SOL–GEL (%)	Gelation (%)	Water uptake (%)
AMPS10–SOLGEL0	10	15	50	0	67	174
AMPS10–SOLGEL10	10	15	50	10	69	169
AMPS10–SOLGEL30	10	15	50	30	73	142
AMPS15–SOLGEL0	15	10	50	0	70	358
AMPS15–SOLGEL30	15	10	50	30	82	206
AMPS20–SOLGEL0	20	5	50	0	69	550
AMPS20–SOLGEL10	20	5	50	10	71	449
AMPS20–SOLGEL20	20	5	50	20	76	255
AMPS20–SOLGEL30	20	5	50	30	81	230
AMPS10-AA0–SOLGEL10	10	0	65	10	70	219
AMPS10-AA0–SOLGEL30	10	0	65	30	78	154

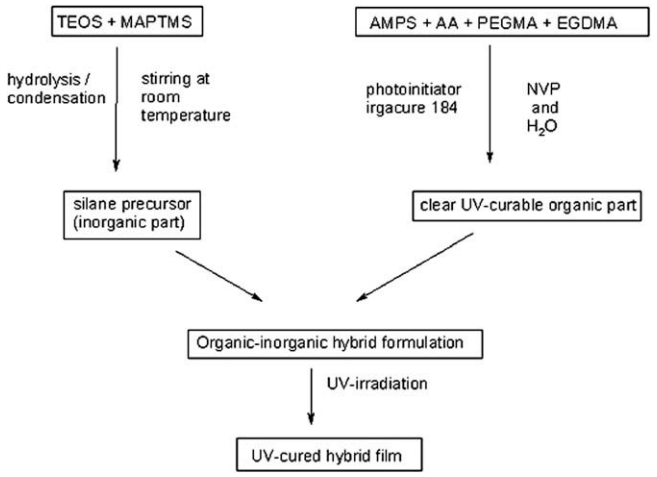

Scheme 1. The preparation procedure of UV curable organic–inorganic hybrid coating.

Thermogravimetric analyses (TGA) of polymers were performed using a TA Instruments Q50 model TGA. Samples were run from 30 to 800 °C at a heating rate of 10 °C min^{-1} under atmospheric conditions.

The morphology of the UV-cured films was examined using scanning electron microscopy (SEM JEOL JSM-6335F). The specimens were prepared for SEM by lyophilization and vacuum drying. The lyophilization was performed at −100 °C for one day and vacuum drying was carried out at 40 °C for one day. The dehydrated samples were placed in liquid nitrogen until the SEM examination, which was performed on the same day. Then an approximately 300 Å gold coating was applied using an Edwards S 150 B sputter coater.

The mechanical properties of the free films were determined by standard tensile stress–strain tests in order to measure the Young's modulus (E), ultimate tensile strength (σ) and elongation at break (ε). Stress–strain tests were performed at room temperature on a Zwick Z010 Universal Tensile Tester using a crosshead speed of 50 mm/min. Reported data is the average of four measurements.

2.5. Differential photocalorimetry

Photopolymerization of the formulations was carried out by a Perkin Elmer Pyris Diamond DSC equipped with an EXFO Omni-Cure™ 2000 photo-DSC accessory. Filtered light (250–450 nm) with an intensity of 20 mW/cm^{-2} at the tip of the light guide was used. Approximately, 100 mg of each sample was placed in the aluminum differential scanning calorimetry (DSC) pans. Heat flow vs. time curves were recorded in an isothermal mode under a nitrogen flow of 20 ml min^{-1} at 37 °C. The rate of reaction in these experiments was calculated by the following equation [20]:

$$R_p = (H/W)/\Delta H \quad (1)$$

where R_p is the rate of polymerization in s^{-1}, H is the heat flow in mW, W is the weight of monomer solution in mg and ΔH is the enthalpy of the material in J g^{-1}.

The heat liberated during the polymerization reaction was directly proportional to the number of vinyl groups reacted in the system. By integrating the area under the exothermic peak, the conversion of the vinyl groups (C) could be calculated by the following equation [21]:

$$C = \Delta H_t/\Delta H_0^{\text{theor}} \quad (2)$$

where ΔH_t is the heat evolved at time t, and $\Delta H_0^{\text{theor}}$ is the theoretical heat for complete conversion [22].

2.6. Water uptake

It is very important to characterize the behavior of proton conducting membranes in contact with water, since the presence of water in the membrane is a prerequisite for reaching high proton conductivity. All of the membranes were soaked in distilled water at room temperature (20.0 ± 0.1 °C) for several days until reaching to constant weight. The swollen membranes were removed from the distilled water, gently wiped with filter paper to remove any water on the surface and weighed (W_s). All of the swollen membranes were kept at 40 °C overnight after which the dried membranes were weighed (W_d). Finally, the water uptake was calculated by using the formula [23]:

$$\text{Water uptake}(\%) = [(W_s - W_d)/W_d] \times 100 \quad (3)$$

All the data reported in this paper is an average of two separate measurements; standard deviations of the measured water uptake were less than 3% of the mean.

2.7. Proton conductivity

The proton conductivity was measured using the AC Impedance Spectroscopy Method in the frequency range from 0.1 Hz to 100 kHz, using a Gamry model potentiostat, and a data acquisition card, type PCI 4750-38064. The proton conductivity was measured under full humidification in a measuring cell [24]. In this case the membranes with an active area of 0.5 × 2 mm were fixed between two platinum electrodes in a Teflon frame and measured in the temperature range from 25 to 50 °C. In all cases three measuring cycles for each material were performed.

The proton conductivity in these experiments was calculated by the following equation [24]:

$$\sigma = d/(t_s w_s R) \quad (4)$$

where d is the distance between the two electrodes, t_s and w_s are the thickness and width of the membrane and R is the resistance value measured.

2.8. Methanol selectivity

Methanol selectivity of the membranes was measured at room temperature using a lab type pervaporation set up. The set up consisted of two reservoirs, each with a capacity of approximately 100 ml, which were separated by a vertical glass tube with a length of 20 cm and a diameter of 0.5 cm. The membrane (AMPS20–SOL-GEL30) to be tested was swollen in methanol:deionized water mixture (90:10 v/v) at room temperature for 24 h, and then was immersed into the left compartment. The vacuum at the permeate side (right compartment) was maintained at 10^{-2} mm Hg using a vacuum pump, and the permeate was collected in a liquid nitrogen trap. Methanol concentration in the permeate was measured by a differential refractive index using an Abbe refractometer (Fisher Scientific) and calculated by using a calibration curve. The methanol selectivity performance of the membrane can be evaluated on the basis of separation factor (α) [25]:

$$\alpha = (PM/PW)/(FM/FW) \quad (5)$$

where PM and PD are the mass fraction of MeOH and water in the permeate, FM and FW are those of MeOH and water in the feed, respectively.

3. Results and discussion

Organic–inorganic hybrid membranes having different compositions of AMPS and AA were prepared, together with the sol–gel-derived silica gel. Membranes were prepared by the UV-curing technique. The feed compositions, percentage gelation and water uptakes are shown in Table 1. In order to remove soluble fractions in UV-cured hybrid films, each sample was extracted in acetone. The gel content of polymeric films was found to be between 67% and 82%. In addition, the photo-DSC was used to follow the rate of polymerization of the photosensitive organic part in the mixture. The reaction heat liberated in the polymerization was directly proportional to the number of vinyl groups reacted in the system. Fig. 1a and b shows the rate of polymerization and double bond conversion vs. time, respectively. As seen in Fig. 1a, all formulations displayed three distinct rates of polymerization stages: initially fast, then leveling off but longer duration and finally decreasing due to the controlled propagation and termination reactions. It was reported previously that the multifunctional monomers exhibit auto-acceleration induced behavior that leads to the very rapid crosslinking process [26].

The conversion profile for AMPS20–SOLGEL10 in Fig. 1b, clearly shows that more than 50% of double bonds undergo polymerization within 1 min. After a fast start, crosslinking reaction slows down and (meth)acrylate conversion levels off at a value of 60%. This effect is attributed to the mobility restrictions appearing upon gelation and ultimately the vitrification of UV-irradiated sample [15,27]. It is very clear from Fig. 1 that, conversion has increased from 60% to nearly 80% with increasing sol–gel content of the membrane. The addition of the sol–gel precursor decreases the viscosity of the growing membrane formulation and this results in an increase of the mobility of the radicalic chains, which may be responsible for the higher conversion. The maximum conversion was obtained for the AMPS20–SOLGEL30 sample. The slight increase in the conversion may also be attributed to the increasing amount of methacrylic groups due to the 3-(methacryloyloxy)propyl trimethoxysilane (MAPTMS).

Fig. 2 shows the ^{29}Si CP/MAS NMR investigation of the AMPS20–SOLGEL30 sample. Mainly, three kinds of signals were observed at −60 ppm ($RSi(OSi)_2(OH)$ or $(RSi(OSi)_2(OCH_2CH_3)$, T^2, −69 ppm ($R Si(OSi)_3$, T^3 and −110 ppm ($Si–(OSi)_4$), Q^4. T^2, T^3 and Q^4 signals give an indication of mostly complete condensation of TEOS and MAPTMS in order to form Si–O–Si bonds of the inorganic constituent. Since MAPTMS monomer has trialkoxy silane functionality at the end group, it should form 100% T^3 species when completely condensed. However, the Q^4 structure indicates that a highly crosslinked inorganic network occurred.

As shown in Table 1, the high water uptake of 174% by the AMPS10–SOLGEL0 membrane could be attributed to its high degree of ionic content. The increase in AMPS content enhances the water uptake and therefore the hydrophilicity of membranes. It is assumed that the increase in water absorption facilitates the proton transfer and thereby increases the proton conductivity in fuel cells. The higher water uptake in membrane depends mainly on sulfonic acid content because the sulfonic acid groups have a strong solvation property [3]. It is well known that, water resides in the hydrophilic domains and facilitates the transport of protons; however, too much water absorption results in the loss of mechanical stability. In this study, the water uptake of the membranes gradually decreases with the addition of sol–gel precursor content. Since MAPTMS acts as a coupling agent between organic and inorganic phases, the incorporation of sol–gel precursor into the organic formulation might result in a crosslinking structure, which was observed with the alteration of solubility behavior of membranes. In addition formation of such a true hybrid system in nanocomposite membrane enhances the membrane stability [28].

The mechanical properties of AMPS based nanocomposite membranes with the sol–gel contents of 0, 10, and 30 wt% are depicted in Table 2. The relatively low Young's modulus and tensile strength values of AMPS10–SOLGEL0 membrane with high elongation at break (65%) reveal that the organic membrane is weak and soft which is typical behavior of hydrogels. However, it was found that the incorporation of sol–gel precursor into membranes increases the Young's modulus effectively. At the same time a decrease in% elongation was also observed. These results

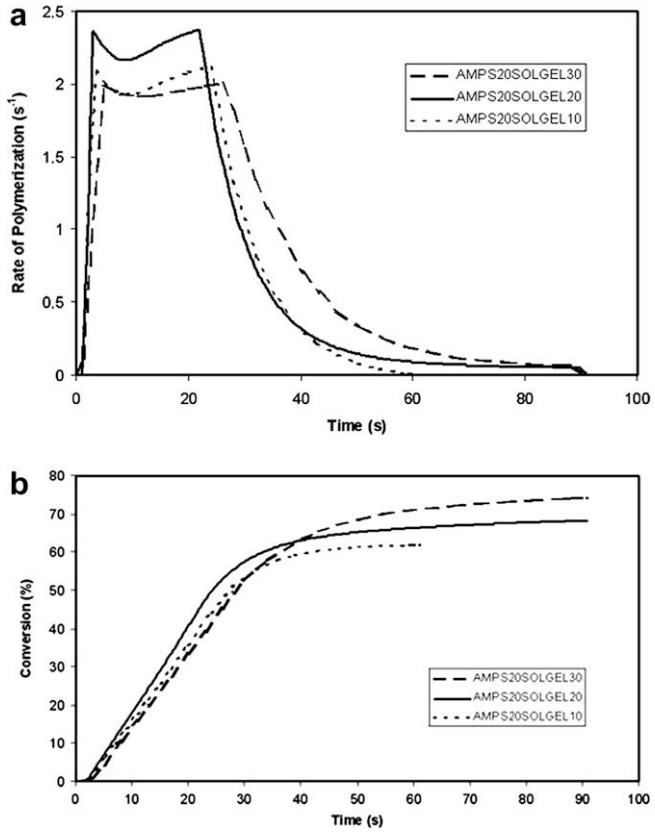

Fig. 1. (a) Rate of polymerization and (b) double bond conversion for compositions having different sol–gel; A: AMPS20–SOLGEL30; B: AMPS20–SOLGEL20, C: AMPS20–SOLGEL10.

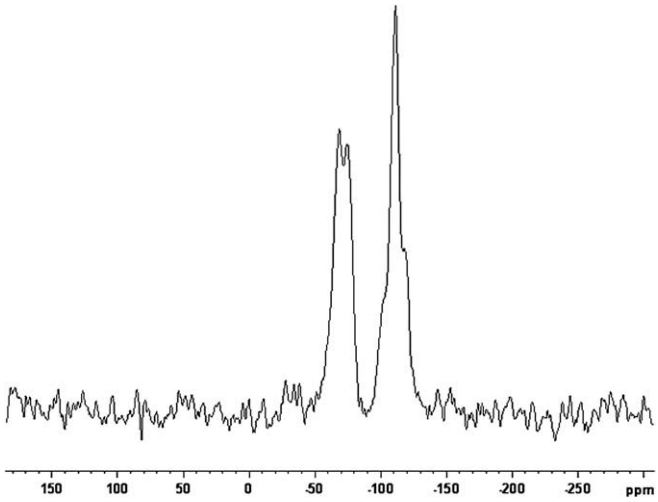

Fig. 2. ^{29}Si NMR spectrum of AMPS20–SOLGEL30 nanocomposite film.

Table 2
The effect of sol–gel precursor content on the stress–strain results of the nanocomposite coatings.

	SOL–GEL (%)	Young modulus (MPa)	Tensile strength (ρ) (MPa)	Elongation-at-break (ε) (%)
AMPS10–SOLGEL0	0	4.3	1.7	65.8
AMPS10–SOLGEL10	10	16.3	3.6	46.2
AMPS10–SOLGEL30	30	110.8	10.7	29.8
AMPS15–SOLGEL0	0	17.7	5.7	98.1
AMPS15–SOLGEL10	10	26.8	7.4	70.4
AMPS15–SOLGEL30	30	37.7	4.4	20.5
AMPS20–SOLGEL10	0	5.7	0.6	34.7
AMPS20–SOLGEL30	30	20.2	4.9	24.9
AMPS10-AA0–SOLGEL10	10	5.1	0.9	23.4
AMPS10-AA0–SOLGEL30	30	20.4	1.3	8.8

demonstrate that, the sol–gel addition into the organic formulation makes the nanocomposite membrane strong and tough. AMPS10–SOLGEL30 membrane has a maximum Young's modulus value of 110.8 MPa. The tensile test also showed that, increasing the sulfonic acid content of the membrane leads to a brittle nature [9]. The comparison between AMPS10–SOLGEL10-30 and AMPS10-AA0–SOLGEL 10–30 samples demonstrated that the acrylic acid incorporation influences the mechanical strength of the membranes. For the AMPS10–SOLGEL30 sample, the modulus is 110.8 MPa and the elongation is 30%; on the other hand for the AMPS10-AA0–SOLGEL 30 sample the modulus decreases to 20.4 MPa and the elongation decreases to 9%. Therefore, the membranes with 0 wt% acrylic acid content were not used due to their poor mechanical properties.

Thermogravimetric analysis (TGA) technique was used to investigate the thermal oxidative stability of nanocomposite membranes. TGA thermograms for AMPS10–SOLGEL0, AMPS10–SOLGEL10 and AMPS10–SOLGEL30 are presented in Fig. 3. The first 10% weight loss, which was observed between 120 and 200 °C is probably due to volatilization of unreacted photoinitiator, reactive diluents or the entrapped moisture present in the film. All samples exhibit a three-step degradation pattern. The first step of degradation is attributed to the decomposition of sulfonic acid groups at approximately 295 °C. The second step indicates the decomposition of the polymer backbone above approximately 390 °C. It has been reported previously that the decomposition temperatures in the range of 250–350 °C is sufficiently high for fuel cell applications [29,30]. Finally the third one, which is observed above 550 °C, indicates complete degraded polymer. From the TGA thermograms, it is clearly observed that the thermal stability of the membranes is improved with the incorporation of sol–gel precursor. As seen in the Table 3, the higher the sol–gel content in the hybrid system, the more char residue is observed. This may be attributed to the sol–gel precursor content in the nanocomposite membrane.

Fig. 4 summarizes the fractured surface morphology of the AMPS10–SOLGEL10 membrane. Secondary electron images (SEI) were applied in SEMs and a highly porous structure is observed in the cross section of the membrane (Fig. 4a). Detailed surface morphology at higher magnification is shown in Fig. 4b. SEM images reveal micro-voids approximately less than 1 μm in diameter. It is known that the pore size is greatly affected by the drying method and freezing rate [31]. In Fig. 5, the comparison between SEM images of vacuum dried and lyophilized membranes can be seen (AMPS20–SOLGEL30). SEM image in Fig. 5a reveals very coarse spherical shaped particles that are homogeneously distributed throughout the fractured surface. The approximate particle size is less than 500 nm. Moreover in the case of the lyophilized sample both surface porosity and dispersed silica gel particles can be seen clearly. In this case silica gel particle size is in the nano-scale (<200 nm).

Proton conductivities of the series of nanocomposite membranes containing AMPS were measured as a function of the weight fraction of AMPS content, weight fraction of sol–gel precursor content and temperature. Proton conductivities increased linearly from 0.033 to 0.094 S cm^{-1} as a function of AMPS content in 30 wt% of sol–gel containing membranes at 25 °C (Fig. 6). All nanocomposite membranes exhibit an increasing conductivity with increasing temperature. In Fig. 7, the effect of sol–gel content on the conductivity of AMPS based nanocomposite membranes is shown. As seen clearly, with the increase in sol–gel content an increase in conductivity was achieved. The proton conductivity of the

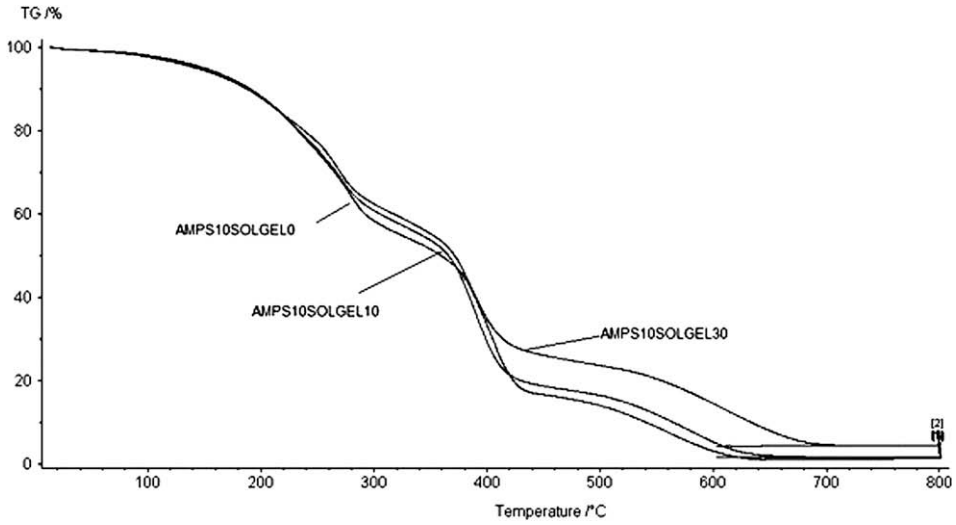

Fig. 3. TGA thermograms for AMPS10–SOLGEL0, AMPS10–SOLGEL10 and AMPS10–SOLGEL30 nanocomposite films.

Table 3
Thermogravimetric analysis of membranes.

	$T_{10\%}$ (°C)	T_{1st} (°C)	T_{2nd} (°C)	T_{3rd} (°C)	Char residuals (wt%)
AMPS10-SOLJEL0	130	250	395	530	1.2
AMPS10-SOLJEL10	118	275	395	550	1.5
AMPS10-SOLJEL30	180	280	390	600	4.2

AMPS20–SOLGEL30 (1.38×10^{-2} S cm^{-1}) was comparable to that of Nafion®-117 (1.52×10^{-2} S cm^{-1}) at 50 °C. Generally, the Grotthus mechanism and vehicle mechanism describe proton diffusion through the membrane [32]. In membranes that support strong hydrogen bonding the Grotthus mechanism is preferred [3]. The proton conductivity of the present membrane did not decrease with increasing temperature due to bound water that acts as media, which supports strong hydrogen bonding.

The methanol selectivity of the AMPS20–SOLGEL30 nanocomposite membrane was measured with a pervaporization test. The selectivity toward methanol and water was found to be 0.032 and 31.25, respectively. The methanol concentration in the permeate side is lower (22/78 v/v) than the feed methanol concentration

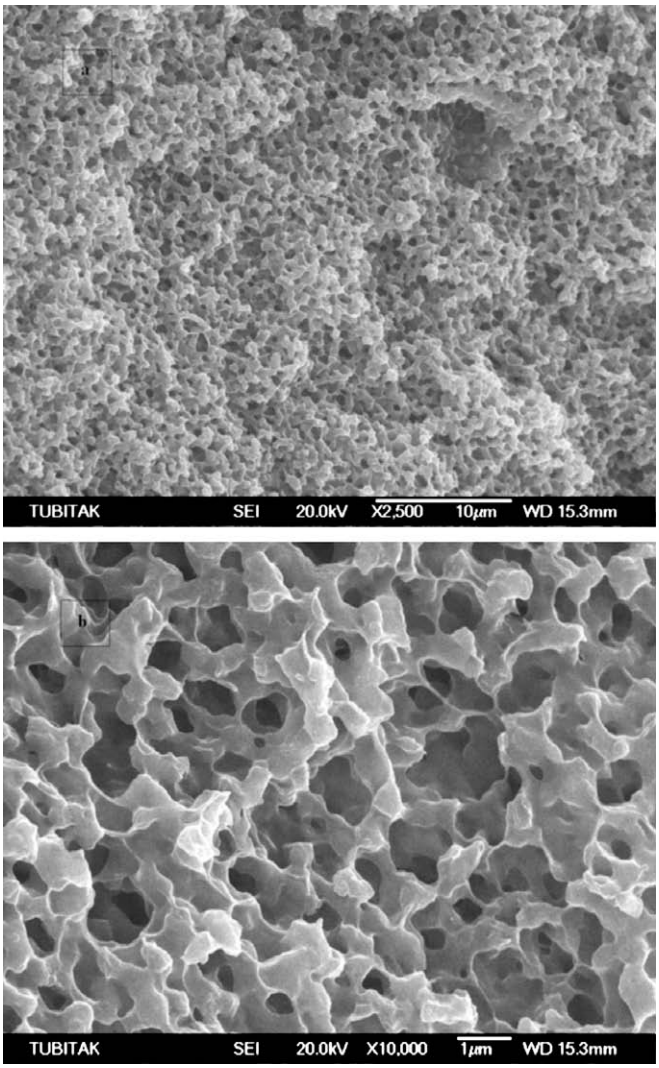

Fig. 4. SEM micrographs of lyophilized AMPS10–SOLGEL10 sample (a) X2500 and (b) X10000 magnification.

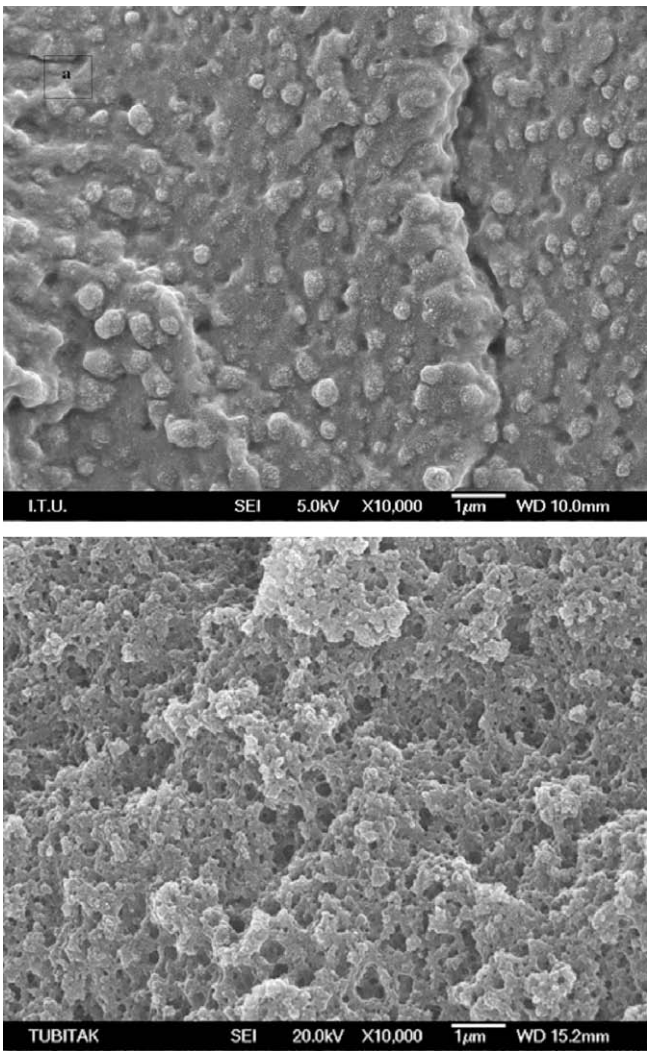

Fig. 5. SEM micrographs of (a) vacuum dried (b) lyophilized AMPS20–SOLGEL30 sample. The original magnifications and size bars are shown in the photomicrographs.

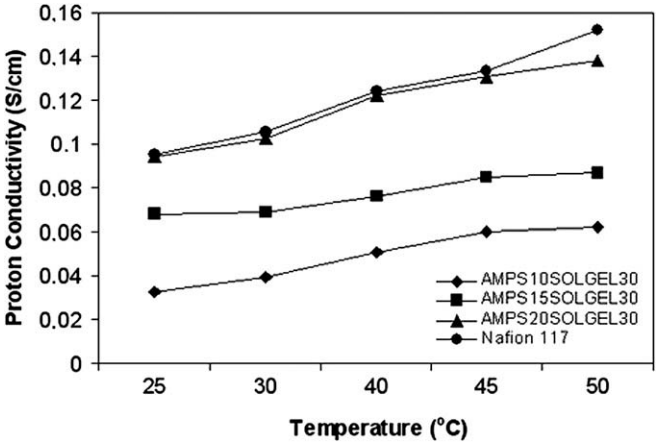

Fig. 6. The effect of AMPS content on the proton conductivities of nanocomposite membranes at various temperatures.

(90/10 v/v), indicating membranes are resistant to methanol permeation. The strong interactions between the organic and inor-

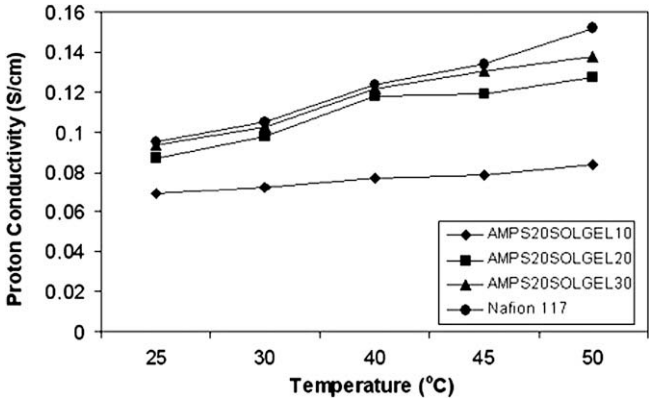

Fig. 7. The effect of sol–gel precursor content on the proton conductivities of nanocomposite membranes at various temperatures.

ganic matrix may suppress polyelectrolyte chain motions and reduce channels so as to lower the methanol diffusion in the membranes [28]. It is also reported that, the lower methanol permeability of hybrid membranes is due to the silica gel particles in the membrane that was used as a methanol barrier by reducing chain mobility and the channel for the passage of methanol molecules [3]. The low methanol solubility in the strongly ionic environment may also affect the methanol permeability.

4. Conclusions

In this study, we first prepared AMPS based UV curable organic/inorganic hybrid membranes. Their water uptake, thermal and mechanical stability and proton conductivity behaviors as well as methanol selectivity were investigated. The water uptake of the membranes increases with an increase of AMPS content. This has been explained with the incorporation of more specific acid groups into the network and consequent greater interaction with water molecules. The photo-DSC experiments showed that approximately 80% of conversion was obtained for AMPS20–SOLGEL30. The ^{29}Si NMR indicated that the inorganic matrix is mostly condensed with T^2, T^3, Q^4 structures. SEM images reveal that a highly porous membrane structure was achieved with homogeneously distributed silica gel domain. The proton conductivity of AMPS20–SOLGEL30 (0.138 S cm^{-1}) was comparable to that of Nafion®-117 (0.152 S cm^{-1}) at 50 °C .The proton conductivities are strongly dependent on the sulfonic acid content and temperature. While the thermal and mechanical properties of the AMPS-containing hybrid membranes are higher, it is noted that they also exhibit low methanol selectivity. It is believed that by further adjustment in the structure of the AMPS based nanocomposite membranes for improving their mechanical strength; they will show a promising application potential for DMFC.

Acknowledgement

This work was supported by Marmara University, Commission of Scientific Research Project under grant Project FEN-A-030108-0014.

References

[1] H. Pei, L. Hong, J.Y. Lee, J. Membrane Sci. 270 (2006) 169–178.
[2] T. Zhang, J. Power Sources 158 (1) (2006) 169–176.
[3] D.S. Kim, H.B. Park, J.W. Rhim, Y.M. Lee, Solid State Ion. 176 (2005) 117–126.
[4] M. Drzewinski, J. Appl. Polym. Sci. 30 (12) (1985) 4753–4770.
[5] M. Rikukawa, K. Sanui, Prog. Polym. Sci. 25 (2000) 1463–1502.
[6] M.A. Hickner, H. Ghassemi, Y.S. Kim, B.R. Einsla, J.E. McGrath, Chem. Rev. 104 (2004) 4587–4611.
[7] H. Munakata, D. Yamamoto, K. Kanamura, J. Power Sources 178 (2008) 596–602.
[8] C.W. Walker Jr., J. Power Sources 110 (2002) 144–151.
[9] H. Pei, L. Hong, L.Y. Lee, J. Power Sources 160 (2006) 949–956.
[10] C.W. Walker Jr., J. Electrochem. Soc. 151 (2004) A1797–A1803.
[11] Y. Shen, J. Xi, X. Qiu, W. Zhua, Electrochim. Acta 52 (2007) 6956–6961.
[12] T. Mitsui, H. Morikawa, K. Kanamura, Electrochemistry 70 (2002) 934–936.
[13] H. Munakata, H. Chiba, K. Kanamura, Solid State Ion. 176 (2005) 2445–2450.
[14] N. Kayaman-Apohan, Z.S. Akdemir, Y. Boztoprak, Macromol. Chem. Phys. 208 (14) (2007) 1572–1581.
[15] M.V. Kahraman, M. Kuğu, Y. Menceloglu, N. Kayaman-Apohan, A. Gungor, J. Non-Cryst. Solids 352 (2005) 2143–2151.
[16] J. Gilberts, A.H.A. Tinnemans, J. Sol–Gel Sci. Technol. 11 (1998) 153–159.
[17] G. Bayramoğlu, M.V. Kahraman, N. Kayaman-Apohan, A. Gungor, Polym. Adv. Technol. 17 (2007) 1–7.
[18] N. Kayaman-Apohan, S. Karatas, B. Bilen, A. Gungor, J. Sol–Gel Sci. Technol. 46 (2008) 87–97.
[19] S. Karatas, C. Kızılkaya, N. Kayaman-Apohan, A. Gungor, Prog. Org. Coat. 60 (2007) 140–147.
[20] E. Oral, N.A. Peppas, Polymer 45 (2004) 6163–6173.
[21] F. Brandl, F. Sommer, A. Goepferich, Biomaterials 28 (2007) 134–146.
[22] E. Andrzejewska, M. Andrzejewski, J. Polym. Sci. Part A: Polym. Chem. 36 (1998) 665–673.
[23] Z.S. Akdemir, H. Akçakaya, M.V. Kahraman, T. Ceyhan, N. Kayaman-Apohan, A. Gungor, Macromol. Biosci. 8 (2008) 852–862.
[24] X. Guo, J. Fang, K. Tanaka, H. Kita, L.-I. Okamoto, J. Polym. Sci. Part A: Polym. Chem. 42 (2004) 1432–1440.
[25] J.H. Chen, Q.L. Liu, J. Fang, A.M. Zhu, Q.G. Zhang, J. Colloid Interf. Sci. 316 (2007) 580–588.
[26] T.F. Scott, W.D. Cook, Polymer 43 (22) (2002) 5839–5845.
[27] K. Studer, C. Decker, E. Beck, R. Schwalm, Prog. Org. Coat. 48 (2003) 92–100.
[28] Y.-H. Su, Y.-L. Liu, Y.-M. Sun, Y.-L. Lai, D.-M. Wang, Y. Gao, B. Liu, M.D. Guiver, J. Membrane Sci. 296 (2007) 21–28.
[29] L.E. Karlsson, P.I. Annasch, J. Membrane Sci. 230 (2004) 61–70.
[30] F. Wang, M. Hickner, Y.S. Kim, T.A. Zawodzinski, J.E. McGrath, J. Membrane Sci. 197 (2002) 231–242.
[31] L.C. Sawyer, D.T. Grubb, Polymer Microscopy, second ed., Chapman and Hall, UK, 1996.
[32] K.D. Kreuer, Chem. Mater. 8 (1996) 610–641.